Gas Phase Stability of Protein Ions in a Cyclic Ion Mobility Spectrometry Travelling Wave Device

Charles Eldrid[1], Jakub Ujma[3], Symeon Kalfas[1], Nick Tomczyk[3], Kevin Giles[3], Mike Morris[3] and Konstantinos Thalassinos[1,2 *]

[1]Institute of Structural and Molecular Biology, Division of Biosciences, University College London, London, WC1E 6BT, UK

[2]Institute of Structural and Molecular Biology, Birkbeck College, University of London, London, WC1E 7HX, UK

[3]Waters Corporation, Wilmslow, SK9 4AX, UK

[*] To whom correspondence should be addressed k.thalassinos@ucl.ac.uk

Abstract

Ion mobility mass spectrometry (IM-MS) allows separation of native protein ions into "conformational families". Increasing the IM resolving power should allow finer structural information to be obtained, and can be achieved by increasing the length of the IM separator. This, however, increases the time that protein ions spend in the gas phase and previous experiments have shown that the initial conformations of small proteins can be lost within tens of milliseconds. Here, we report on investigations of protein ion stability using a multi-pass travelling wave (TW) cyclic IM (cIM) device. Using this device, minimal structural changes were observed for Cytochrome C after hundreds of milliseconds, while no changes were observed for a larger multimeric complex (Concanavalin A). The geometry of the instrument (Q-cIM-ToF) also enables complex tandem IM experiments to be performed which were used to obtain more detailed collision induced unfolding pathways for Cytochrome C. The novel instrument geometry provides unique capabilities with the potential to expand the field of protein analysis via IM-MS.

Introduction

The invention of soft-ionisation techniques[1–3] has allowed the transfer of intact biomolecules and proteins into the gas phase.[4–6] Early electrospray mass spectrometry experiments (ESI-MS) showed pronounced differences in charge state distribution depending on the solution conditions suggesting that solution phase protein structure can be probed using ESI-MS.[7] In their landmark work, Clemmer and Jarrold constructed an ESI – ion mobility – mass spectrometer (ESI-IM-MS) which revealed that

a single charge state of a protein can be present in a range of conformations.[8] This sparked a significant interest in studies of proteins in the gas phase. IM-MS has the advantage of being able to detect multiple and lowly populated conformational ensembles from small sample volumes, which are comparable to those seen in solution when the ions have a low internal energy (E_{int}).[9] Being able to detect these conformational states provides information on protein folding dynamics, and requires far lower sample concentrations when compared to other structural techniques such as X-ray crystallography and NMR. Introduction of the first mainstream commercial IM-MS instrumentation (Synapt HDMS, Waters Corporation, 2006)[10] accelerated implementation of the technique in protein studies. IM-MS has been used to show the basic dynamic behaviour of proteins,[11–13] protein domain organisation[14] and to identify and investigate the structural dynamics of disordered proteins.[15,16] Deliberate activation of ions through increasing the internal energy via collisional heating can cause unfolding,[17] which can provide important information on the structural stability of proteins under different conditions or with different states, the effect of modifications or ligands on protein structure and dynamics,[16,18,19] and the subunit organisation of oligomers.[19,20] This can also be applied to protein complexes to investigate oligomerisation pathways and subunit organisation of complexes.[12,21–24]

IM-MS functions by introducing analyte ions into a drift-cell containing an inert buffer gas such as helium or nitrogen. Ions drift through the cell under the influence of an electric field and collide with buffer gas molecules. Drift velocity of ions is governed by their mobility which is inversely proportional to their collision cross-section (CCS). Species which are extended (larger CCS), will undergo a greater number of collisions with the buffer gas and have a longer drift time compared to more compact species (smaller CCS). Mass to charge ratios (*m/z*) are then measured for each ion by a mass spectrometer.

Increasing the resolving power of the IM device should *in principle* enable separation of overlapping features allowing greater understanding of protein structures in the gas phase. The resolving power of the IM device depends on the temperature, ion charge, electric field and on the path length.[25] There are several examples in the literature where attempts were made to increase the resolving power of the IM apparatus by decreasing the temperature,[26,27] increasing the electric field[28] and increasing the path length.[29,30] Conventionally, the latter is a physical distance that ions travel, and thus a number of several meters long drift tube (DT) type instruments have been realised.[29,30] There are practical limits in this approach related to the physical size of the apparatus and high voltages required. Alternatively, an experimental setup with inverted "frame of reference" can be envisaged where the ions are trapped in a stream of moving gas by an opposing electric field; as in the case of trapped ion mobility spectrometry technique (TIMS).[31] Here, the "effective path length" can be influenced by a separation time scale and gas velocity. Another way of achieving long separation path is to utilise multi-pass devices. The cyclotron mobility spectrometer described by Glaskin *et al.*, uses a drift cell made of 4 curved segments which are joined by ion funnels[32] which re-focus ions.[29] Electric field applied to

subsequent segments/funnels is switched; only the ions with mobilities resonant with the field switching frequency can proceed to the following segments while others are lost. An IM spectrum is obtained by scanning the field switching frequency. Several developments of high resolution IM instrumentation have been facilitated by travelling wave (T-Wave, TW) technology[33] which relies on a series of voltage pulses which propel ions across the device. T-Wave technology eliminates problems related to high voltages, required for the traditional, linear field DT-IM apparatus. A T-Wave based, multi-pass separator (cyclic IM) was first introduced by Giles *et al.*,[34] and separation at path length over 50m was demonstrated.[35] Further advances in a T-Wave technology include structures for lossless ion manipulation (SLIM), notably by Smith *et al*.[36]A multi-pass SLIM device has allowed IM separations over an extremely long path length (~1km).[37] Other recent developments in IM technology include tandem methods. Two-stage IM technique was first presented by Koeniger *et al.*[38,39] where an instrument featuring two drift tubes allowed separation in the first IM stage, mobility selection, activation *and* separation of product ions in the second stage. This was further expanded to three-stage IM method by Merenbloom *et al.*[40] More recently, the multi-stage IM technology was combined with a multi-pass cyclic IM separator by Giles *et al.*,[35] allowing for IMS^n – type workflows.

Increasing the resolution of IM separation via path length *typically* increases experiment time scales. Understandably, changes in the nature of analyte ions occurring on the time scale of separation are undesirable. Previous work by Badman *et al.*, showed that Cytochrome C ions underwent structural changes with time.[41,42] Utilising a quadrupole ion trap (QIT) – IM – MS instrument, ions were stored for varying amounts of time in the QIT, prior the IM-MS measurement. The structural changes started occurring at approximately 30 ms, and had stabilised after 60 ms, showing that the initial population of +7 to +10 ions contain precursors or conformational intermediates that unfold in the gas phase.[41] Similar results were reported for ubiquitin.[43] It was suggested that solution specific conformations transform to new gas phase structures in the absence of solvent after a period of 30 milliseconds. More recently, Allen *et al.* has utilised a SLIM based tandem IM instrument[44] to study the Cytochrome C ions. It was shown that structural changes occurred an order of magnitude later than reported previously. This was attributed primarily to the pressure related differences in effective ion temperatures[45] in the QIT and tandem IM systems and also solution dependent effects, further confirmed by collision-induced unfolding (CIU) experiments.[44] Collectively, the previous work suggests that IM separation timescale appropriate for native protein ions is likely to be on the order of tens to hundreds milliseconds. Importantly, Badman *et al.* and Allen *et al.* both utilised a relatively short, linear field DT devices where transit times are on the order of tens of milliseconds. Moreover, due to a relatively low velocity of ions in such devices, their effective temperatures are essentially equal to that of the buffer gas. The latter is not necessarily the case in the T-Wave based IM separation. It was reported previously that ion heating during the T-Wave based IM separation can

cause some structure perturbation, the effect being especially pronounced for low molecular weight, high mobility species.[46,47] The native protein ions typically have relatively low charge and high mass, thus representing a contrasting case *in principle*. Nevertheless, it is of interest and importance to evaluate the extent of native structure perturbation upon prolonged exposure to T-Waves, particularly in relation to possibility of high-resolution IM separations in the future.

Here, we utilise a prototype cyclic IM-MS instrument enabling custom experiments designed to further explore the stability of monomeric (Cytochrome C, β-Lactoglobulin) and multimeric (Concanavalin A) proteins, in a T-Wave based separator. While all proteins were electrosprayed from solutions conductive to native type analyses, Cytochrome C was also sprayed from a denaturing solution, replicating the original experiments performed by Badman *et al.*[41] Ions were subjected to trapping in the RF ion guide (Pre-Store, Figure 1) and native conformations were found to be stable for hundreds of milliseconds. Additional experiments were also performed to show that extended time within the cyclic ion guide under typical separation conditions does not significantly impact protein structure in the gas phase. IMS-CIU-IMS experiments revealed detailed unfolding pathways for Cytochrome C. Our results agree with previous reports suggesting that the native like conformation or proteins is maintained in the gas phase under extended time scales, and for the first time show that this is also true within a cyclic T-Wave device. We also show that the solution conditions have a strong influence on the evolution of gas phase conformations. Collectively our data show that the cyclic-IM instrument can be used for studying protein dynamics, stability and unfolding in the gas-phase.

Methods

Sample preparation

The proteins (equine Cytochrome C (Merck Millipore, UK), β-Lactoglobulin (Sigma, UK) and Concanavalin A (Sigma, UK) were buffer exchanged into 49/49/2 (v/v %) water/methanol/acetic acid (WMA) or 200 mM ammonium acetate solution (AmAc) using 3, 10 or 30 kDa Amicon Ultra 0.5 mL centrifugal spin filters (Merck Millipore, UK). The samples were spun a total of three times at 12,000 rpm, for 15 minutes at room temperature. The protein was then diluted to 8 - 10 μM after concentration calculation using a Qubit protein assay (ThermoFisher Scientific, UK).

Mass Spectrometry

The samples were introduced into the instrument using a nano-ESI source (Waters Corp., Wilmslow, UK). The emitters (manufactured using a P97 Flaming/Brown micropipette puller, coated in gold using a Quorum Q150R S sputter coater) were held at 1.2 kV. The cIM instrument design is discussed in detail elsewhere (manuscript in preparation) and so will only be briefly covered here. The

instrument schematic is presented in Figure 1. Ions are transferred from the source through the first vacuum stages using ion guide arrangements (StepWave), which propel ions towards the quadrupole mass filter. The subsequent trap cell is used for accumulating and bunching ions prior to IM separation. The resulting ion packets are then injected into a helium cell. In this work we utilise the He cell injection energy to generate some of the collisional induced unfolding (CIU) data. The subsequent ion guide (Pre-Store) operates in Nitrogen and guides the ions into the a multi-function array (Figure 1C) of electrodes forming part of an orthogonal closed loop, the cIM separator (98 cm path length, single pass resolution of ~65). The IMS pressure was held at 2.2 mbar and the T-wave height was 40 V. The T-Wave direction in the array can be altered to either match those in the cIM device (i.e. separate) or to inject/eject ions from it. The control software GUI enables creation of custom sequences of functions to facilitate selective ejection of ions from cyclic IM device and/or activation followed by further separation of product ions. The typical sequence of events employed in single/ multi-pass experiments is presented in Figure S1. Post cIM, ions are transported through an ion guide (Post-Store) and on to the ToF via a segmented quadrupole (XS) transfer cell. The transfer cell allows activation of mobility separated ions. The oa-ToF features an offset V geometry allowing *m/z* measurements at resolutions in excess of 60,000 FWHM.[35] Instrument control and data acquisition is via a flexible, web-based GUI.

In addition to a typical single/multi-pass operation (Figure S1), three custom modes of operation were designed to explore protein stability in the gas phase. Firstly, in the "trapping" mode ions are stored in the pre-store guide for a prolonged period of time, before IM separation takes place (Figure S2). This mode enables the time-resolved assesment of the protein conformation stability in absence of any (intentional) activation. Secondly, the "spinning" mode was designed to verify the effect of ion heating during the T-Wave based IM separation (Figure S3). Normally, the number of passes around the cIM (and hence separation time) is limited by so-called wrap-around – a phenomenon where the fastest ions ultimately catch up with the slowest ones. To extend the exposure to T-Waves, ions are passed around the cIM device for varying amounts of time (allowing wrap-around) before being re-collected in the pre-store and subjected to another IM separation before detection. Lastly, the IMS-CIU-IMS mode of operation is used (Figure S4). Here, a mobility-selected ion population can be collected in the pre-store while the remaining ions are removed from the cIM. Selected ions are then re-injected into the array at increased energies and activation occurs. This way, we can probe unfolding transitions of selected regions of arrival time space, increasing the specificity of CIU experiments.[18,48] In this work we focus on the dual stage method, however, multi-stage experiments (IMS^n) can be performed in an analogous way.

Data Analysis

Data were analysed using Masslynx v4.1 (Waters Corporation) and Driftscope v2.1 (Waters Corporation). CIU fingerprint plots were created using Benthesikyme.[49] Population fitting was performed using *in-house* software written in Python 2.7, peak maxima were identified using the second derivative and manually adjusted to ensure the same conformational populations were tracked across the different experiments. Each conformational family was approximated by a Gaussian distribution. The sum of all distributions was optimised to produce the best fit to the experimental data. No restraint to the full width half maximum value of each Gaussian was imposed like in previous work.[49] The code is freely available at https://github.com/ThalassinosLab/CIVU.

Results

Cytochrome C in Denaturing Solution

An extended charge state distribution was observed for CytC (WMA) (see figure 2A), indicative of an unfolded protein, as has been previously recorded in low pH solutions.[50] Charge states +7, +9 and +11 were isolated via quadrupole for further experimentation (Figure 3A-C and Figure S5). The arrival time distribution (ATD) of the +7 (Figure 3A) represents a single conformational family, with a small, lower mobility 'tail'. During trapping, unfolded populations are apparent at 120 ms and increase in intensity with time. A similar effect is seen when the +7 ions spend the equivalent amount of time in the cIM guide exposed to T-Waves (Figure 3B, S8B). The +9 charge state appears to be more prone to unfolding in spinning mode with the application of the T-wave (Figure S5D-F, S9B). Nevertheless, the magnitude of this effect is relatively small, equivalent to less than 5 V of activation (Figure 3C). ATDs of +11 (Figure S5G-I) do not appear to contain the native, compact population. Instead intermediate and unfolded populations are observed. Interestingly, these ions show minimal change upon trapping/spinning suggesting these conformations are not perturbed in the gas phase (Figure S10A, B).

Cytochrome C in Native Solution

CytC in 200 mM ammonium acetate was also analysed, and a very narrow charge state distribution was observed, with high abundance of the +7 charge state (Figure 2B). Other charge states ranging from +8 to +5 could be seen at low abundance. Minimal activation upon both trapping and spinning experiments was observed for the +7 (Figure 3D – E), similar to the CytC WMA +7 (Figure 3A – B and S11A, B). Again, comparing these structural transitions to the CytC AmAc +7 CIU plots (Figure 3F), they are equivalent to less than 5 V of activation.

In direct comparison with CytC WMA +7 the ATDs show that CytC AmAc +7 has a lower proportion of extended species (Figure S11) and these appear to undergo gas phase transitions over longer time-scales. CIU analysis of the quadrupole isolated +7 ions revealed that they unfold more readily when

originating from a solution of WMA than AmAc. This shows that protein stability in the gas phase is related to that of the solution structure, as also shown previously.[44]

β-Lactoglobulin

β-Lactoglobulin (βLac) is a 16 kDa protein, with several disulphide bridges, that exists as a monomer and dimer in solution; ratio being dependent on protein concentration and the ionic strength of the solution.[51] βLac was detected mainly as monomer (Figure 2C), and the charge states +7 to +9 were quadrupole isolated for further analysis. The +7 charge state did not display structural changes upon trapping or spinning (Figures S6A–C and S12), however, the +8 and +9 charges displayed very minimal structural changes over the course of 240 ms (Figure 3G-I, S13 and S14) comparable to 10 - 20 V of intentional activation (Figure S6I).

Concanavalin A

To investigate the effect of prolonged gas phase exposure on the stability of multimeric complexes we analysed Concanavalin A (ConA), a protein which exists as a 51 kDa dimer or 102 kDa tetramer. The mass spectrum of ConA contained monomeric, dimeric and tetrameric species, with the most intense peaks belonging to the dimeric states (Figure 2D). The tetrameric +21 charge state was quadrupole isolated for further analysis. Here, no structural perturbation upon trapping or spinning (Figure 3J – L, S15) was observed. In addition, no complex dissociation was observed, apart from under deliberate activation conditions (Figure S7). The CIU experiments revealed that minimal conformational changes were observed at up to 50 V activation (Figure 3L).

Increased Resolution

Multi-pass cIM separation offers increased resolution as a function of the square root of the number of passes, n ($\sqrt{(nz)}$, where z is the ion charge state).[34] The above experiments have shown that extended time in both the pre-store and, when under T-Wave motion in the cIM, can cause small conformational changes for some protein ions, but not others, and this appears to be strongly related to mass and charge state. The +7 charge state ions of CytC generated from ammonium acetate were subjected to 1, 2 and 4 passes around the cyclic ion guide (Figure 4).

Subjecting the +7 ions to higher resolution separation did not reveal new features in the ATD (Figure 4A – C). This suggests that the initial width of the protein ATD is due to the extremely large variety of highly similar conformational families, unresolvable by the cIM separator operating at resolution of ~350 at 4 passes. This, however, is not always the case and is most likely protein, charge state, and solution condition specific. For example, early experiments with bovine insulin ions (generated from denaturing solution) showed that increased number of passes allows greater resolution of previously unresolvable features (Figure S16).

As an alternative approach to probe the presence of structural sub-populations in more detail, we used an IMS-CIU-IMS approach.

IMS-CIU-IMS

An experiment which can be performed on this instrument is multi-stage IMS (IMS^n), where a subset ion population can be selected after IM separation, activated and subjected to IM separation again. Due to the geometry of the instrument this can theoretically be done a limitless number of times. Here we will focus our attention on phenomena that can be probed in more detail compared to a traditional single stage collision induced unfolding (CIU) analysis. As an example, we use the quadrupole isolated, +7 ion of CytC which was subjected to activation in the trap at (20 V). The initial ATD is presented in Figure 5A. We then use the IMS-CIU-IMS methodology to obtain unfolding profiles of 4 subsets of this initial population (B-E). Conformation α, upon activation, directly converts into conformations β, γ and δ. As longer drift time conformations are selected, populations β to δ are directly accessed. This clearly shows the directionality of unfolding events. Two conformations (ε and ζ) which are not present in the initial ATD appear after the extension of conformation δ, between 60 – 80 V of activation.

Discussion

Our data show that proteins can to a large extent retain their native and multimeric states within the time scales compatible with high resolution IM separations. Importantly, the effect of prolonged exposure to T-waves appears, in most cases, similar to trapping alone, indicating little structural perturbation induced by T-wave based separation itself. In this study we explored the time scales up to 360 ms which would typically exceed the realistic time scales for separation of protein ions. These time scales (and number of passes around the device) are limited by wrap-around in the present setup. The aforementioned CytC work by Allen *et al.*,[44] explored time scales up to 33 seconds which at the moment is beyond the scope of our work. The magnitude of change observed in several hundred milliseconds region by Allen *et al*. agrees well with data presented here. This is an order of magnitude longer than reported previously by Badman *et al.*[39] This is most likely due to the fact that the quadrupole ion trap (QIT) used by to retain the protein ions for increments of time, operated at a much lower pressure, approximately 0.0133 mbar[41,42] compared to ~2.2 mBar in the cIM device and the ~5 mBar used in the SLIM based tandem IM.

In line with previous work we observe differences in CIU profiles of CytC generated from native and denaturing solutions during single stage CIU analysis.[44] We also highlight that CytC ions generated from denaturing solution show lower gas phase stability during trapping and spinning experiments

compared to ions generated from native solution. Like in Allen *et al.*, Cyt C ions from native solutions retained initial conformations for much longer time periods and appeared to transition into more extended structures at around 200 ms.

The loss of native conformation is less apparent for larger proteins. For βLac, the lowest charge state observed (+7) did not undergo any detectable change. Higher charge states (+8, +9) were minimally perturbed, and only after 240 ms. This is in agreement with previous reports showing that low charge states are more reflective of the solution conformation of proteins.[52] No loss of initial conformations was observed for ConA. This suggests that the gas phase longevity of the native structures is proportional to the ion mass and, most likely, inversely proportional to its charge. CytC may indeed be particularly sensitive to gas phase studies as previous work showed that while it does not undergo backbone changes, the surface residues are rearranged[53–55] and it retains fewer salt-bridges when in the gas-phase rather than in solution.[56] Gas-phase salt-bridges are thought to play a very important role in the retention of native or native-like states, due to the much lower electrostatic permittivity of the vacuum compared to that of aqueous solution.[57–59] Interestingly, subjecting native protein ions to an increased number of passes around the cIM device did not resolve overlapping features, suggesting that the ATDs of native ions consist of a very large number or even a continuum of conformers.[39] This is perhaps not so surprising, if we imagine, for example, a variety of ways in which solvent exposed residues of the protein can be re-arranged during desolvation. This observation is somehow parallel with the previous findings from the study utilising variable temperature IM instrumentation,[26] where only a minimal increase of resolution was observed for native protein ions at cryogenic temperatures. Collectively, this suggests that the native protein ATDs are naturally broad not due to diffusion or interconversion but inherent conformational heterogeneity. The above phenomena will be investigated in the future work utilising the high resolution capabilities of the instrument combined with the IMS-CIU-IMS methodology presented here.

Acknowledgements

Charles Eldrid is funded by a BBSRC iCASE award with Waters BB/L015382/1.

1. Hillenkamp, F., Karas, M., Beavis, R. C. & Chait, B. T. Matrix-Assisted Laser Desorption/Ionization Mass Spectrometry of Biopolymers. *Analytical Chemistry* **63**, 1193A–1203A (1991).

2. Yamashita, M. & Fenn, J. B. Electrospray Ion-Source - Another Variation on the Free-Jet Theme. *J. Phys. Chem.* **88**, 4451–4459 (1984).

3. Fenn, J. B. Electrospray ionization mass spectrometry: How it all began. *J. Biomol. Tech.* **13**, 101–118 (2002).

4. Siuzdak, G. *et al.* Mass spectrometry and viral analysis. *Chem. Biol.* **3**, 45–48 (1996).

5. Ruotolo, B. T. *et al.* Biochemistry: Evidence for macromolecular protein rings in the absence of bulk water. *Science (80-.).* **310**, 1658–1661 (2005).

6. Dole, M. *et al.* Gas phase macroions. *Macromolecules* **1**, 96–97 (1968).

7. Chowdhury, S. K., Katta, V. & Chait, B. T. Probing Conformational Changes in Proteins by Mass Spectrometry. *J. Am. Chem. Soc.* **112**, 9012–9013 (1990).

8. Clemmer, D. E., Hudgins, R. R. & Jarrold, M. F. Naked Protein Conformations: Cytochrome c in the Gas Phase. *J. Am. Chem. Soc.* **117**, 10141–10142 (1995).

9. Chen, S. H. & Russell, D. H. How Closely Related Are Conformations of Protein Ions Sampled by IM-MS to Native Solution Structures? *J. Am. Soc. Mass Spectrom.* **26**, 1433–1443 (2015).

10. Pringle, S. D. *et al.* An investigation of the mobility separation of some peptide and protein ions using a new hybrid quadrupole/travelling wave IMS/oa-ToF instrument. *Int. J. Mass Spectrom.* **261**, 1–12 (2007).

11. Shelimov, K. B., Clemmer, D. E., Hudgins, R. R. & Jarrold, M. F. Protein structure in Vacuo: Gas-phase conformations of BPTI and cytochrome c. *J. Am. Chem. Soc.* **119**, 2240–2248 (1997).

12. Wojnowska, M. *et al.* Autophosphorylation activity of a soluble hexameric histidine kinase correlates with the shift in protein conformational equilibrium. *Chem. Biol.* **20**, 1411–1420 (2013).

13. Pacholarz, K. J. & Barran, P. E. Distinguishing Loss of Structure from Subunit Dissociation for Protein Complexes with Variable Temperature Ion Mobility Mass Spectrometry. *Anal. Chem.* **87**, 6271–6279 (2015).

14. Zhong, Y., Han, L. & Ruotolo, B. T. Collisional and coulombic unfolding of gas-phase proteins: High correlation to their domain structures in solution. *Angew. Chemie - Int. Ed.* **53**, 9209–9212 (2014).

15. Beveridge, R. *et al.* A mass-spectrometry-based framework to define the extent of disorder in proteins. *Anal. Chem.* **86**, 10979–10991 (2014).

16. Dickinson, E. R. *et al.* Insights into the Conformations of Three Structurally Diverse Proteins: Cytochrome c, p53, and MDM2, Provided by Variable-Temperature Ion Mobility Mass Spectrometry. *Anal. Chem.* **87**, 3231–3238 (2015).

17. Clemmer, D. E. & Jarrold, M. F. Ion mobility measurements and their applications to clusters and biomolecules. *J. Mass Spectrom.* **32**, 577–592 (1997).

18. Nyon, M. P. *et al.* An integrative approach combining ion mobility mass spectrometry, X-ray crystallography, and nuclear magnetic resonance spectroscopy to study the conformational dynamics of α1-antitrypsin upon ligand binding. *Protein Sci.* **24**, 1301–1312 (2015).

19. Landreh, M. *et al.* Integrating mass spectrometry with MD simulations reveals the role of lipids in Na+/H+ antiporters. *Nat. Commun.* **8**, 13993 (2017).

20. Hyung, S. J., Robinson, C. V. & Ruotolo, B. T. Gas-Phase Unfolding and Disassembly Reveals Stability Differences in Ligand-Bound Multiprotein Complexes. *Chem. Biol.* **16**, 382–390 (2009).

21. Benesch, J. L. P. Collisional Activation of Protein Complexes: Picking Up the Pieces. *J. Am. Soc. Mass Spectrom.* **20**, 341–348 (2009).

22. Bernstein, S. L. *et al.* Amyloid-β 2 protein oligomerization and the importance of tetramers and dodecamers in the aetiology of Alzheimer's disease. *Nat. Chem.* **1**, 326–331 (2009).

23. Bleiholder, C., Dupuis, N. F., Wyttenbach, T. & Bowers, M. T. Ion mobilityg-mass spectrometry reveals a conformational conversion from random assembly to β-sheet in amyloid fibril formation. *Nat. Chem.* **3**, 172–177 (2011).

24. Eschweiler, J. D., Rabuck-Gibbons, J. N., Tian, Y. & Ruotolo, B. T. CIUSuite: A Quantitative Analysis Package for Collision Induced Unfolding Measurements of Gas-Phase Protein Ions. *Anal. Chem.* **87**, 11516–11522 (2015).

25. Louis, R. H., Hill, H. H. & Eiceman, G. A. Ion Mobility Spectrometry in Analytical Chemistry. *Crit. Rev. Anal. Chem.* **21**, 321–355 (1990).

26. Ujma, J., Giles, K., Morris, M. & Barran, P. E. New High Resolution Ion Mobility Mass Spectrometer Capable of Measurements of Collision Cross Sections from 150 to 520 K. *Anal. Chem.* **88**, 9469–9478 (2016).

27. May, J. C. & Russell, D. H. A mass-selective variable-temperature drift tube ion mobility-mass spectrometer for temperature dependent ion mobility studies. *J. Am. Soc. Mass Spectrom.* **22**, 1134–1145 (2011).

28. Dugourd, P., Hudgins, R. R., Clemmer, D. E. & Jarrold, M. F. High-resolution ion mobility measurements. *Rev. Sci. Instrum.* **68**, 1122 (1998).

29. Glaskin, R. S., Ewing, M. A. & Clemmer, D. E. Ion trapping for ion mobility spectrometry measurements in a cyclical drift tube. *Anal. Chem.* **85**, 7003–7008 (2013).

30. Merenbloom, S. I., Glaskin, R. S., Henson, Z. B. & Clemmer, D. E. High-resolution ion cyclotron mobility spectrometry. *Anal. Chem.* **81**, 1482–1487 (2009).

31. Silveira, J. A., Michelmann, K., Ridgeway, M. E. & Park, M. A. Fundamentals of Trapped Ion Mobility Spectrometry Part II: Fluid Dynamics. *J. Am. Soc. Mass Spectrom.* **27**, 585–595 (2016).

32. Shaffer, S. A., Prior, D. C., Anderson, G. A., Udseth, H. R. & Smith, R. D. An Ion Funnel Interface for Improved Ion Focusing and Sensitivity Using Electrospray Ionization Mass Spectrometry. *Anal. Chem.* **70**, 4111–4119 (1998).

33. Giles, K. *et al.* Applications of a travelling wave-based radio-frequency-only stacked ring ion guide. *Rapid Commun. Mass Spectrom.* **18**, 2401–2414 (2004).

34. Giles, K. *et al.* 62nd ASMS Conference on Mass Spectrometry and Allied Topics. in *Baltimore, MD. June* 15–19 (2014).

35. Giles, K. *et al.* Design and Performance of a Second-Generation Cyclic Ion Mobility Enabled Q-ToF. *65th ASMS Conference on Mass Spectrometry and Allied Topics* 2017 (2017).

36. Webb, I. K. *et al.* Experimental evaluation and optimization of structures for lossless ion manipulations for ion mobility spectrometry with time-of-flight mass spectrometry. *Anal. Chem.* **86**, 9169–9176 (2014).

37. Deng, L. *et al.* Serpentine Ultralong Path with Extended Routing (SUPER) High Resolution Traveling Wave Ion Mobility-MS using Structures for Lossless Ion Manipulations. *Anal. Chem.* **89**, 4628–4634 (2017).

38. Koeniger, S. L. *et al.* An IMS-IMS analogue of MS-MS. *Anal. Chem.* **78**, 4161–4174 (2006).

39. Koeniger, S. L. & Clemmer, D. E. Resolution and Structural Transitions of Elongated States of Ubiquitin. *J. Am. Soc. Mass Spectrom.* **18**, 322–331 (2007).

40. Merenbloom, S. I., Koeniger, S. L., Valentine, S. J., Plasencia, M. D. & Clemmer, D. E. IMS-IMS and IMS-IMS-IMS/MS for separating peptide and protein fragment ions. *Anal. Chem.* **78**, 2802–2809 (2006).

41. Badman, E. R., Hoaglund-Hyzer, C. S. & Clemmer, D. E. Monitoring Structural Changes of Proteins in an Ion Trap over 10 - 200 ms: Unfolding Transitions in Cytochrome c Ions. *Anal. Chem.* **73**, 6000–6007 (2001).

42. Badman, E. R., Myung, S. & Clemmer, D. E. Evidence for unfolding and refolding of gas-phase cytochrome c ions in a Paul trap. *J. Am. Soc. Mass Spectrom.* **16**, 1493–1497 (2005).

43. Myung, S., Badman, E. R., Lee, Y. J. & Clemmer, D. E. Structural transitions of electrosprayed ubiquitin ions stored in an ion trap over ~10 ms to 30 s. *J. Phys. Chem. A* **106**, 9976–9982 (2002).

44. Allen, S. J., Eaton, R. M. & Bush, M. F. Structural Dynamics of Native-Like Ions in the Gas Phase: Results from Tandem Ion Mobility of Cytochrome c. *Anal. Chem.* **89**, 7527–7534 (2017).

45. Viehland, L. A. & Mason, E. . Gaseous ion mobility and diffusion in electric fields of arbitrary strength. *Ann. Phys. (N. Y).* **110**, 287–328 (1978).

46. Morsa, D., Erie Gabelica, V. & De Pauw, E. Effective Temperature of Ions in Traveling Wave Ion Mobility Spectrometry. *Anal. Chem* **83**, 7 (2011).

47. Merenbloom, S. I., Flick, T. G. & Williams, E. R. How hot are your ions in TWAVE ion mobility spectrometry? *J. Am. Soc. Mass Spectrom.* **23**, 553–562 (2012).

48. Tian, Y., Han, L., Buckner, A. C. & Ruotolo, B. T. Collision Induced Unfolding of Intact Antibodies: Rapid Characterization of Disulfide Bonding Patterns, Glycosylation, and Structures. *Anal. Chem.* **87**, 11509–11515 (2015).

49. Sivalingam, G. N., Cryar, A., Williams, M. A., Gooptu, B. & Thalassinos, K. Deconvolution of ion mobility mass spectrometry arrival time distributions using a genetic algorithm approach: Application to α1-antitrypsin peptide binding. *Int. J. Mass Spectrom.* **426**, 29–37 (2018).

50. Chowdhury, S. K., Katta, V. & Chait, B. T. Probing Conformational Changes in Proteins by Mass Spectrometry. *J. Am. Chem. Soc.* **112**, 9012–9013 (1990).

51. Sakurai, K., Oobatake, M. & Goto, Y. Salt-dependent monomer-dimer equilibrium of bovine β-lactoglobulin at pH 3. *Protein Sci.* **10**, 2325–2335 (2008).

52. Scarff, C. A., Thalassinos, K., Hilton, G. R. & Scrivens, J. H. Travelling wave ion mobility mass spectrometry studies of protein structure: biological significance and comparison with X-ray crystallography and nuclear magnetic resonance spectroscopy measurements. *Rapid*

Commun. Mass Spectrom. **22**, 3297–3304 (2008).

53. Breuker, K. & McLafferty, F. W. Native Electron Capture Dissociation for the Structural Characterization of Noncovalent Interactions in Native Cytochrome c. *Angew. Chemie - Int. Ed.* **42**, 4900–4904 (2003).

54. Breuker, K. & McLafferty, F. W. The thermal unfolding of native cytochrome c in the transition from solution to gas phase probed by native electron capture dissociation. *Angew. Chemie - Int. Ed.* **44**, 4911–4914 (2005).

55. Steinberg, M. Z., Elber, R., McLafferty, F. W., Gerber, R. B. & Breuker, K. Early structural evolution of native cytochrome c after solvent removal. *ChemBioChem* **9**, 2417–2423 (2008).

56. Zhang, Z., Browne, S. J. & Vachet, R. W. Exploring salt bridge structures of gas-phase protein ions using multiple stages of electron transfer and collision induced dissociation. *J. Am. Soc. Mass Spectrom.* **25**, 604–613 (2014).

57. Bonner, J., Lyon, Y. A., Nellessen, C. & Julian, R. R. Photoelectron Transfer Dissociation Reveals Surprising Favorability of Zwitterionic States in Large Gaseous Peptides and Proteins. *J. Am. Chem. Soc.* **139**, 10286–10293 (2017).

58. Konermann, L. Addressing a Common Misconception: Ammonium Acetate as Neutral pH "Buffer" for Native Electrospray Mass Spectrometry. *J. Am. Soc. Mass Spectrom.* **28**, 1827–1835 (2017).

59. Porrini, M. *et al.* Compaction of Duplex Nucleic Acids upon Native Electrospray Mass Spectrometry. *ACS Cent. Sci.* **3**, 454–461 (2017).

Figures

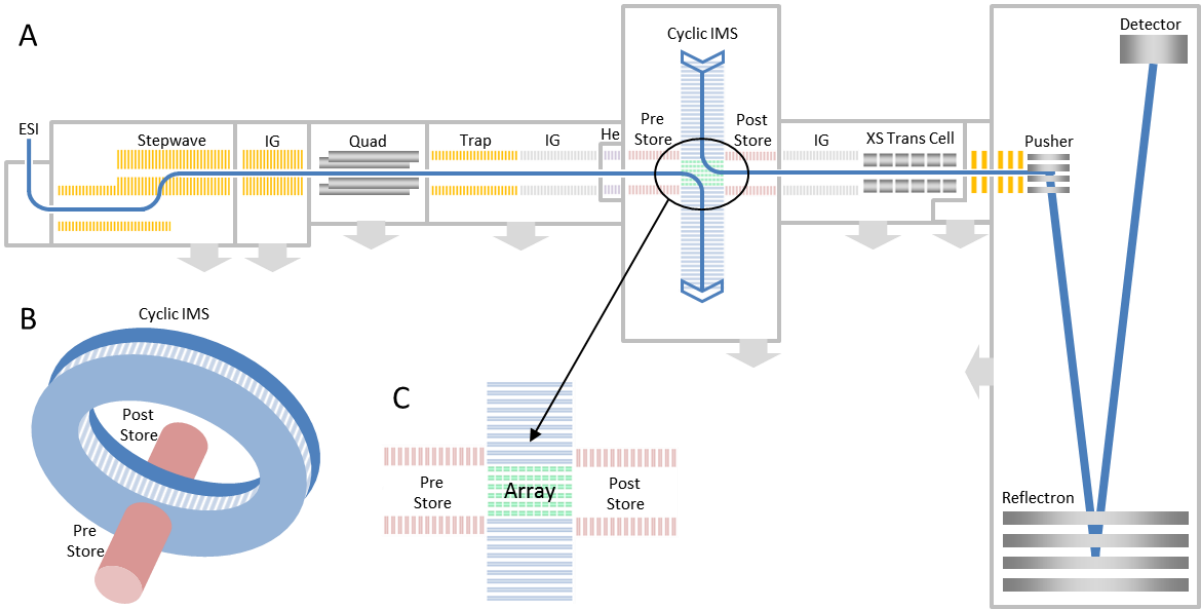

Figure 1 Instrument schematic showing the Q-cIM-ToF geometry. B: Cartoon showing orthogonal arrangement of Cyclic IMS and neighbouring ion optics. C: Multi-function region. Reproduced with permission from Ujma *et al.,* submitted.

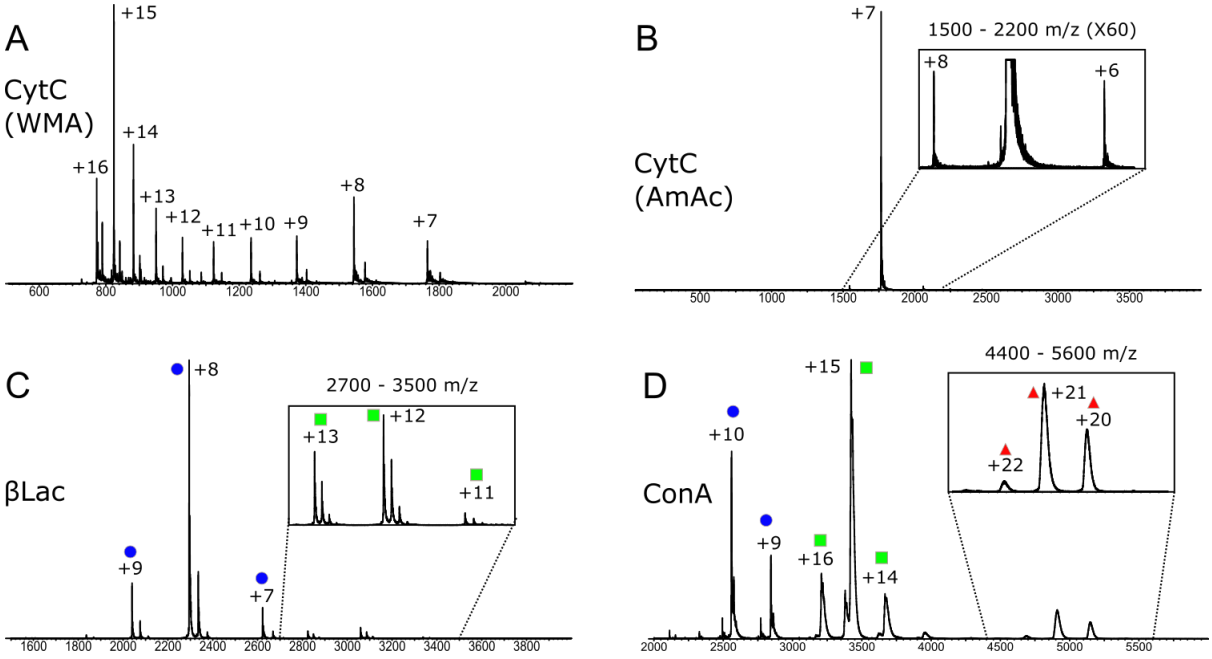

Figure 2 Mass spectra for the proteins (A) Cytochrome C (CytC) in acid (WMA) and (B) ammonium acetate (AmAc), (C) β-Lactoglobulin (βLac) and (D) Concanavalin A (ConA). Blue circle = monomer, green square = dimer, red triangle = tetramer.

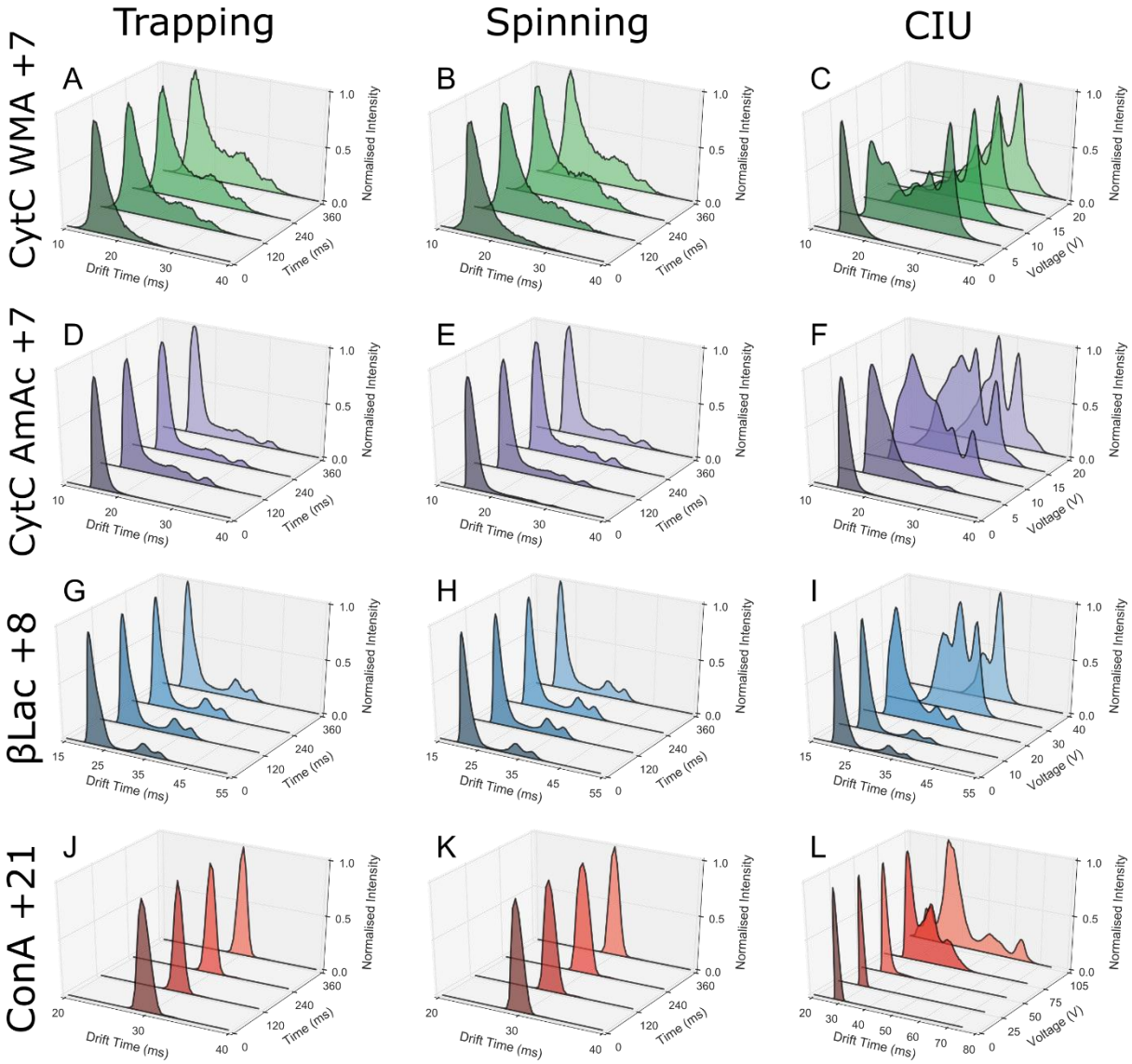

Figure 3 Trapping (A, D, G, J), spinning (B, E, H, K) and CIU (C, F, I, L) experiments shown for CytC +7 WMA (A - C, green), CytC +7 AmAc (D - F, purple), βLac +8 (G - I, blue), ConA +21 (J - L, red). Each figure is composed of ATD slices, arranged in increasing experimental increment, *i.e.* trapping time (ms), from dark to light shading. Plotted is the drift time against normalised intensity.

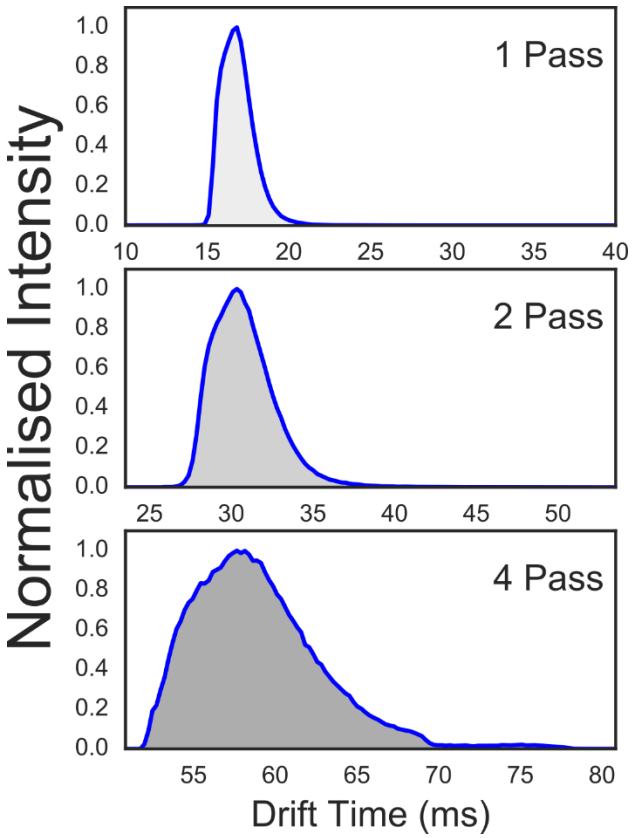

Figure 4 CytC (AmAc) +7 charge state arrival time distribution after multiple passes of the cyclic drift-region 1, 2 and 4 passes in the cIM.

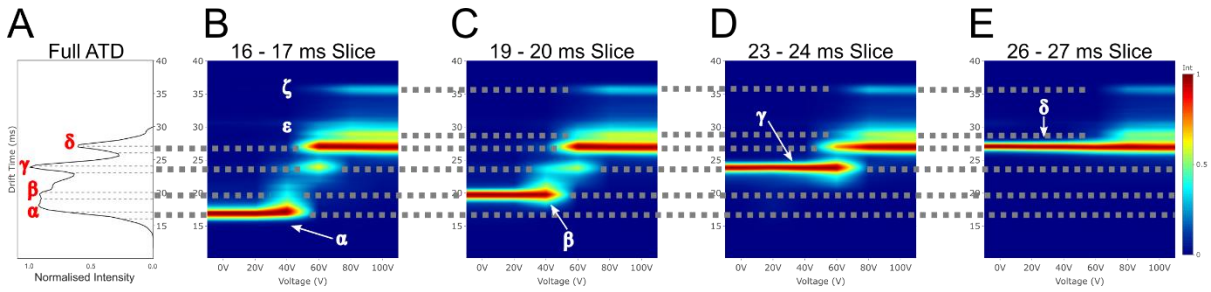

Figure 5 Slice CIU for an activated +7 CytC ion. A) arrival time distribution, with the slices which have been removed for further mobility selection bounded by dotted lines B – E) CIU fingerprints for slices 16-17, 19-20, 23-24, 26-27 ms. Notable populations labelled as α, β, γ, δ, ε and ζ.

Supplementary Figures

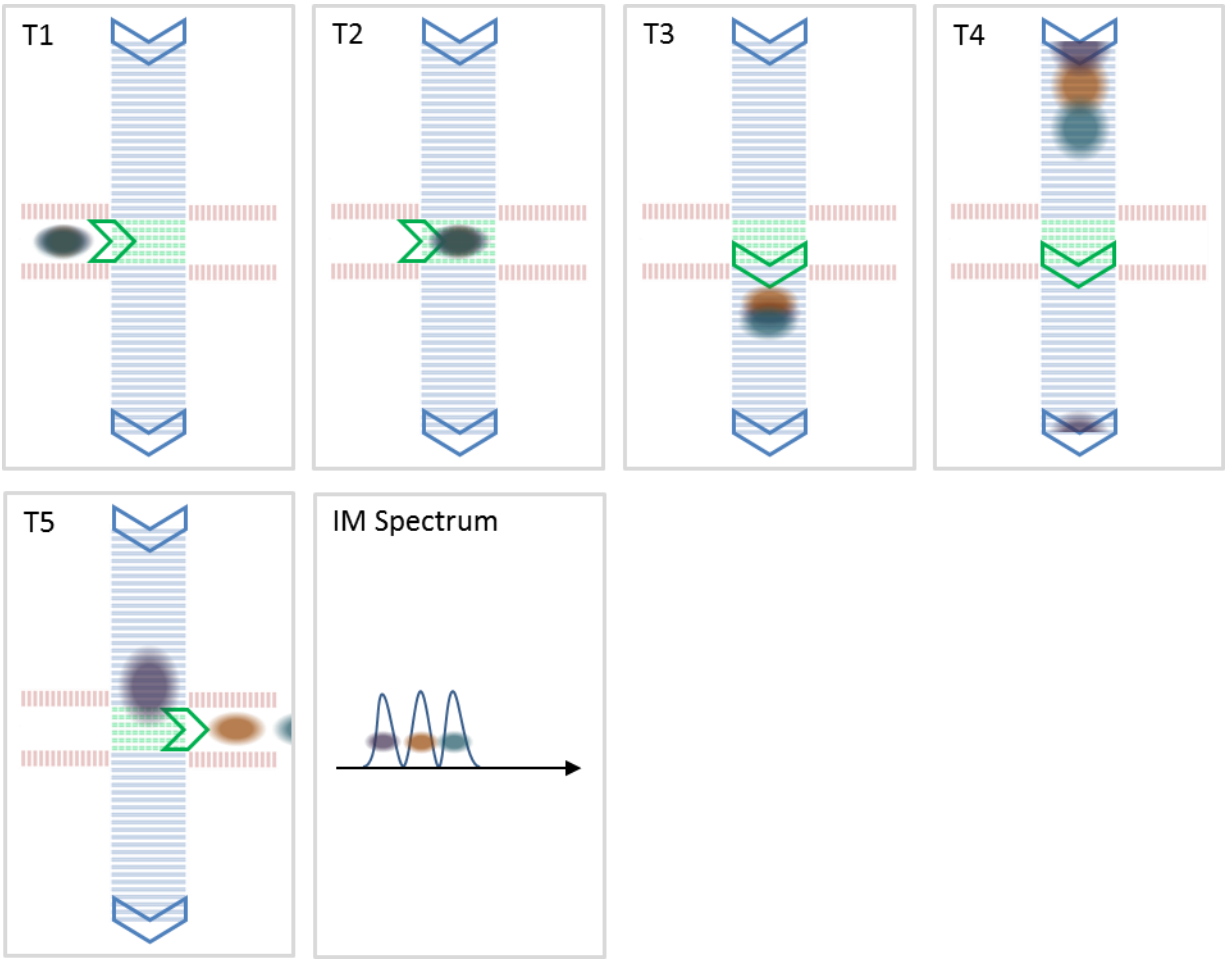

Figure S1. Events in single/multipass IMS operation. Time points 1 and 2 (T1 and T2): ions are injected from store (red) into the array (green). T3: direction of T-waves in the array (green arrow) changes to match those in cIM region (blue arrows); ions begin to drift around the cIM device. T4: after a certain number of passes three species appear separated. T5: Ions are ejected to the ToF and IM-MS spectrum is recorded.

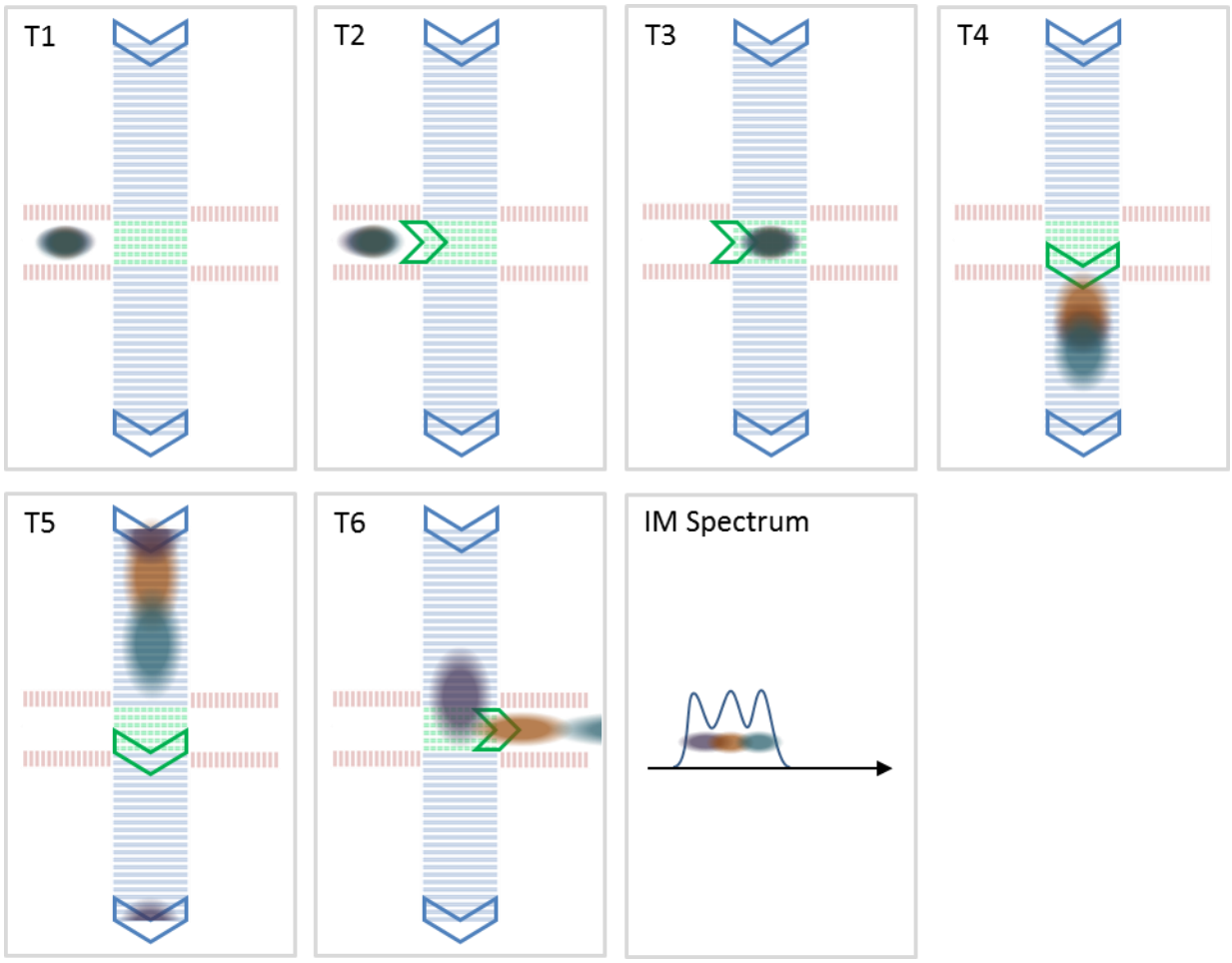

Figure S2. Events in "trapping" mode of operation. Before IM separation takes place, ions are trapped for a prolonged period of time in the pre array store (T1). Steps T2-T6 correspond to T1-T5 steps in the Figure S1. The obtained IM spectrum is directly comparable to that in the Figure S1.

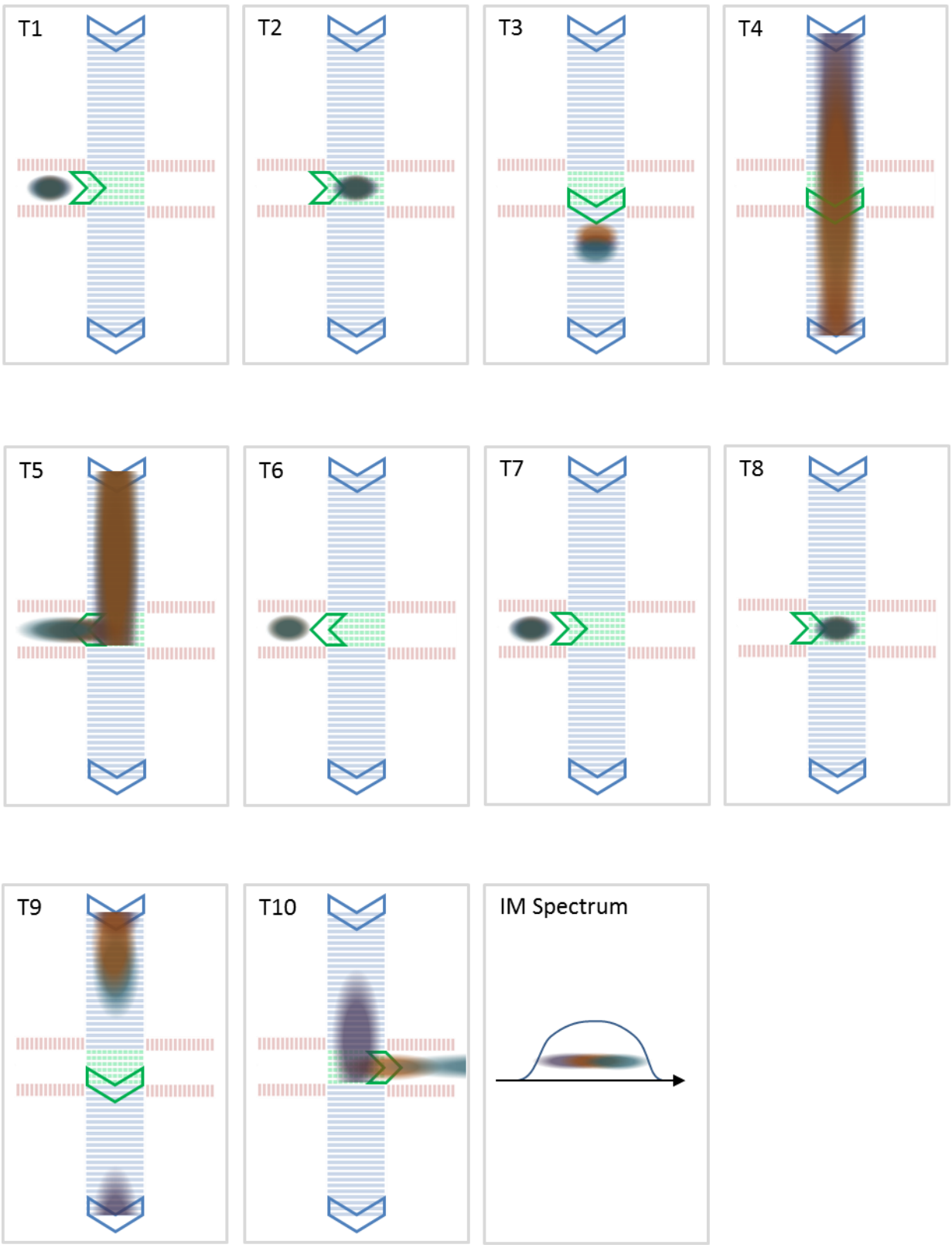

Figure S3. Events in "spinning" mode of operation. Time points T1-T3: ions are injected from store (red) into the array and IM separation takes place. T4: ions are passed around beyond the wrap around limit (i.e. time when fastest ions overtake the slowest ones). T5: ions are recollected in pre array store. T6-T10: ions are re-injected into the array and IM separation of ions that have been "spun" for prolonged period of time is performed. The obtained IM spectrum is directly comparable to that in the Figure S1.

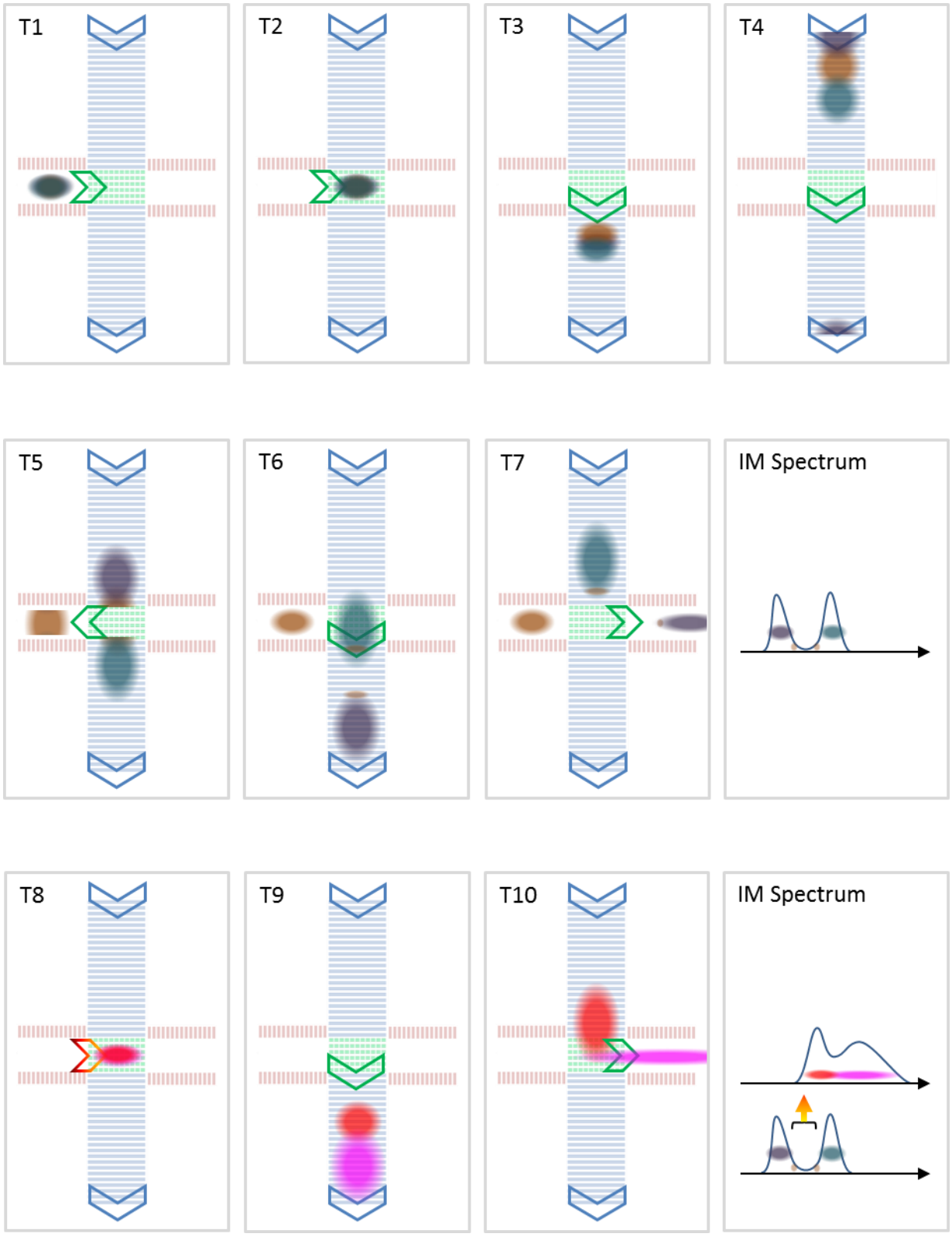

Figure S4. Events in IMS^2 mode of operation. Time points 1 and 2 (T1 and T2): ions are injected from store (red) into the array (green). T3: direction of T-waves in the array (green arrow) changes to match those in cIM region (blue arrows); ions begin to drift around cIM device. T4: after certain number of passes three species appear separated. T5: IM selection; as brown population of ions drifts through the array region, the array T-wave direction changes and the selected ion population is ejected into the store. T6, T7: ions remaining in the cIM travel for an additional pass around cIM before being ejected out. T8: ions from the store are re-injected into the array at high energy and form product ions. T9: Product ions (originating from brown precursor population) are mobility separated.

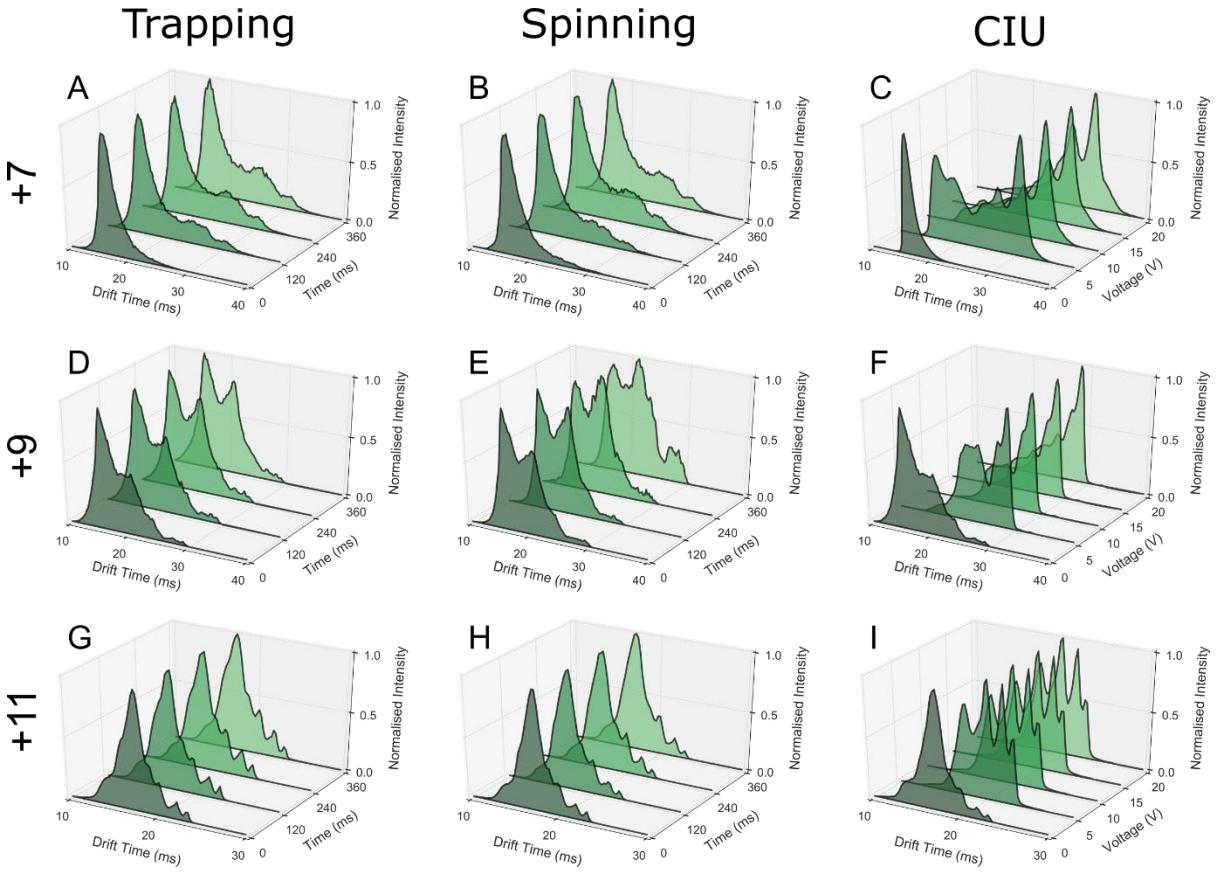

Figure S5 Trapping (A, D, G), spinning (B, E, H) and CIU (C, F, I) experiments for Cytochrome C in WMA, from quadrupole isolated +7 (A - C), +9 (D - F) and +11 (G - I) charge states. Each figure is composed of ATD slices, arranged in increasing experimental increasing experimental increment, *ie.* trapping time (ms), from dark to light shading. Plotted is the drift time against normalised intensity.

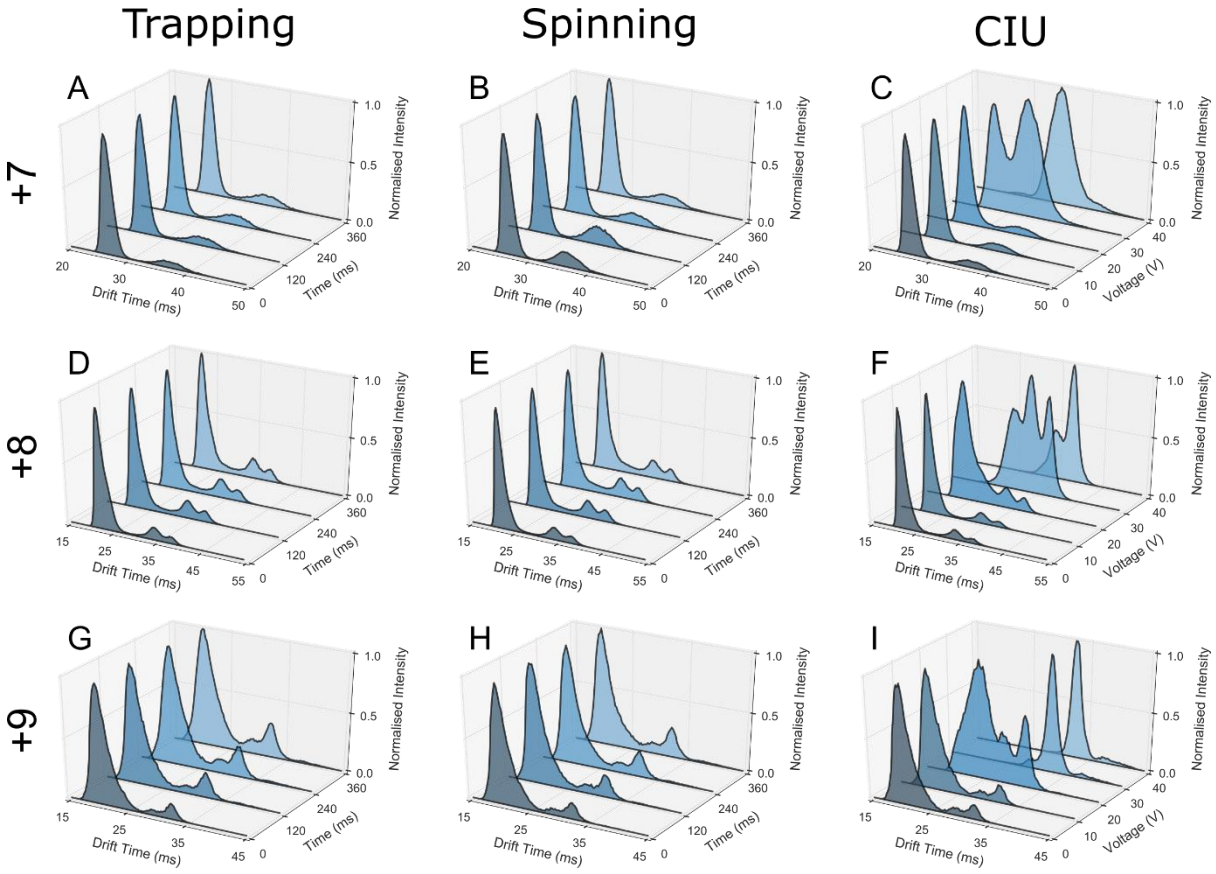

Figure S6 Trapping (A, D, G), spinning (B, E, H) and CIU (C, F, I) experiments for β-Lactoglobulin, from quadrupole isolated +7 (A - C), +8 (D - F) and +9 (G - I) charge states. Each figure is composed of ATD slices, arranged in increasing experimental increment, *ie*. trapping time (ms), from dark to light shading. Plotted is the drift time against normalised intensity.

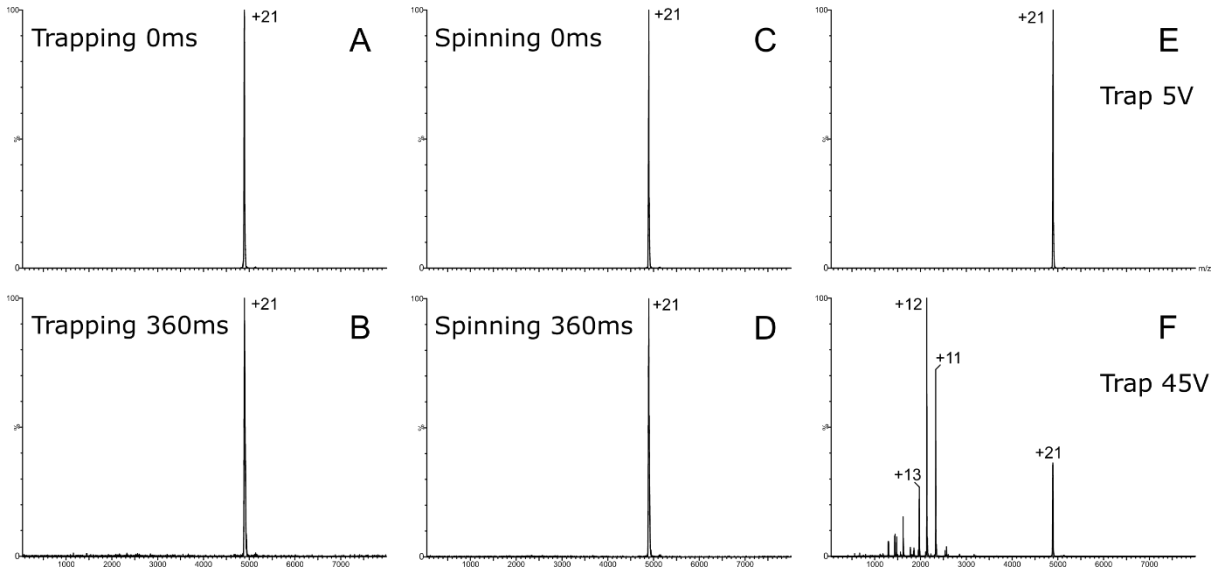

Figure S7 Mass spectra for the quadrupole isolated +21 charge state of Concanavalin A during initial (A, C, E) and final (B, D, F) increments of trapping (A – B), spinning (C – D) and CIU (E – F) experiments. Main peaks annotated. At high voltage during the CIU experiments the tetrameric +21 state decays dissociates into monomeric charge state distribution of +13 to +11. Spectra smoothed with a mean window of 5, twice.

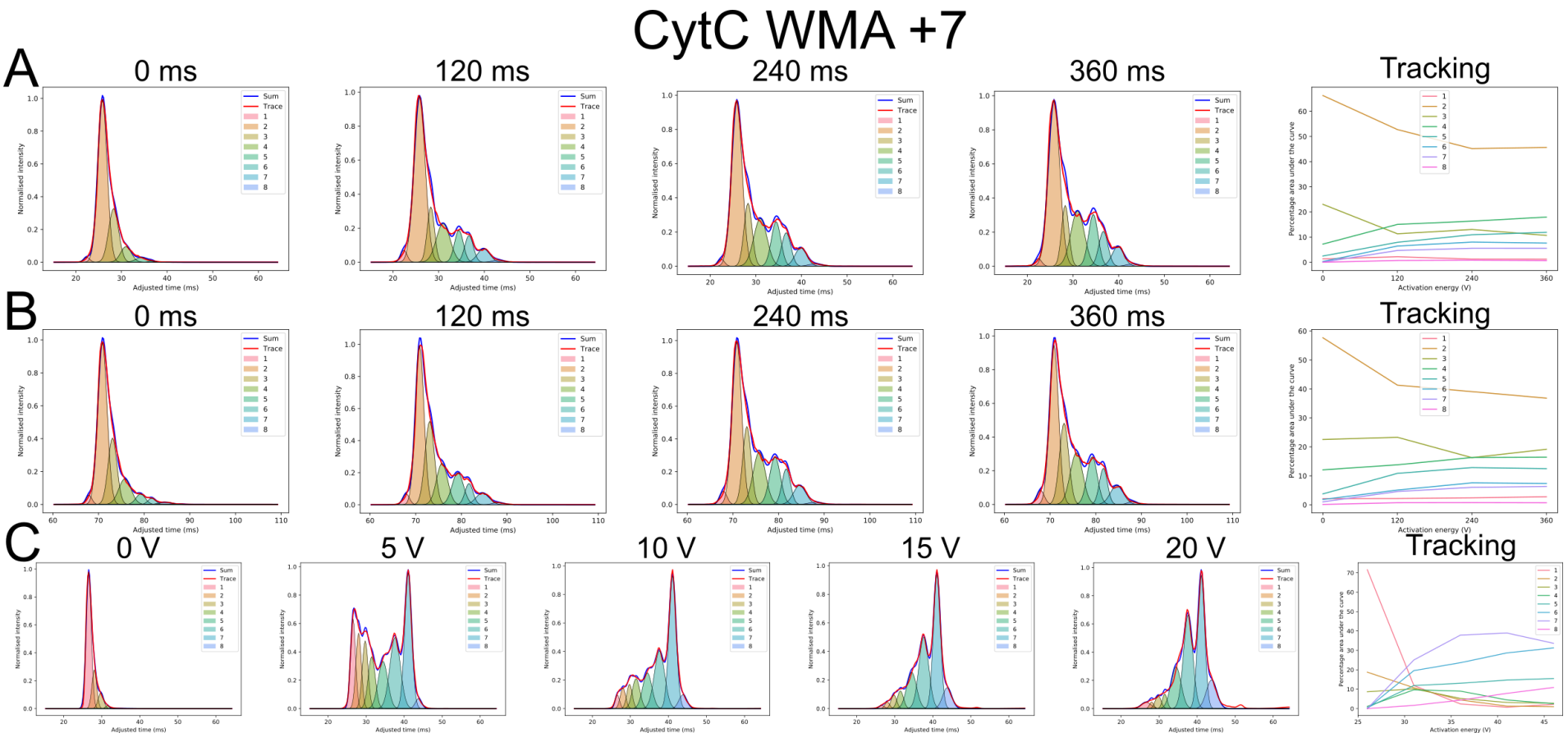

Figure S8 Population tracking for CytC WMA +7 experiments A) tracking B) spinning C) CIU

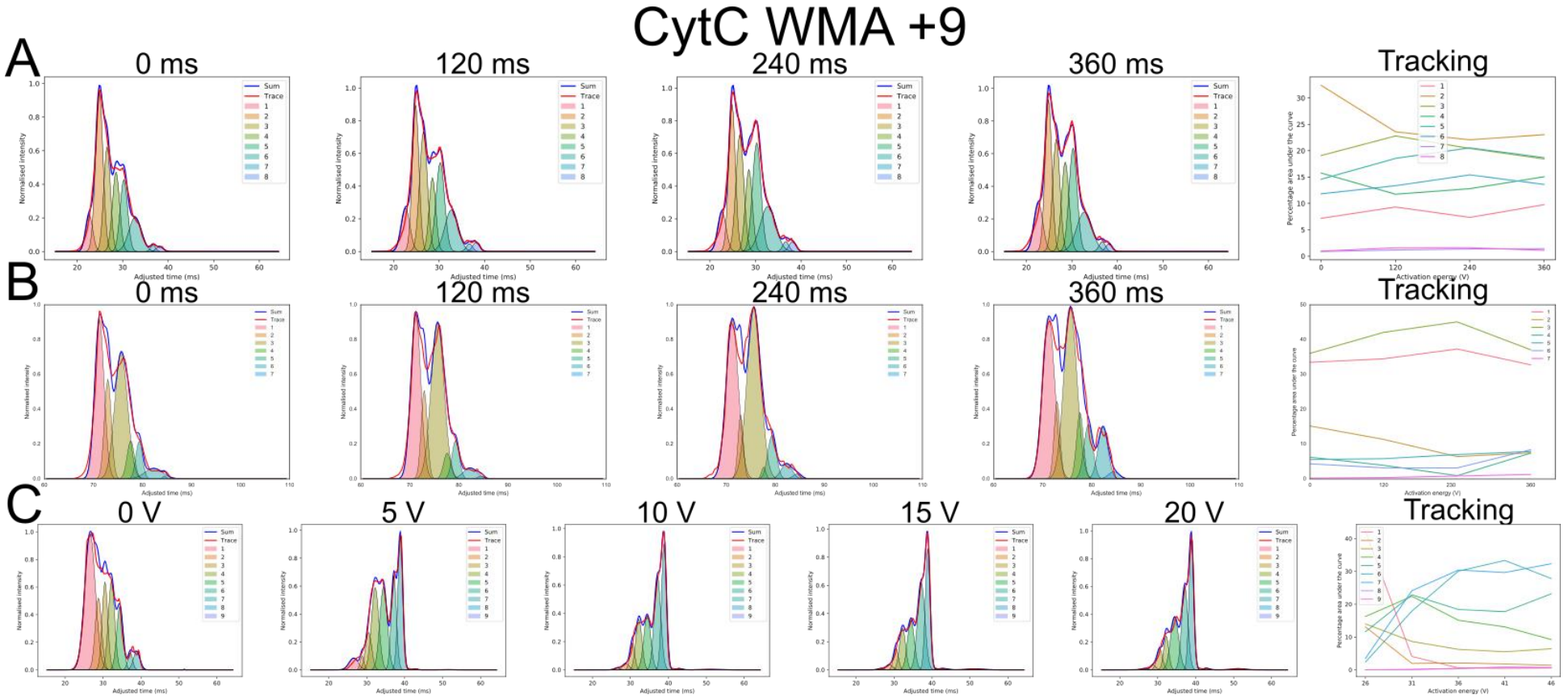

Figure S9 Population tracking for CytC WMA +9 experiments A) tracking B) spinning C) CIU

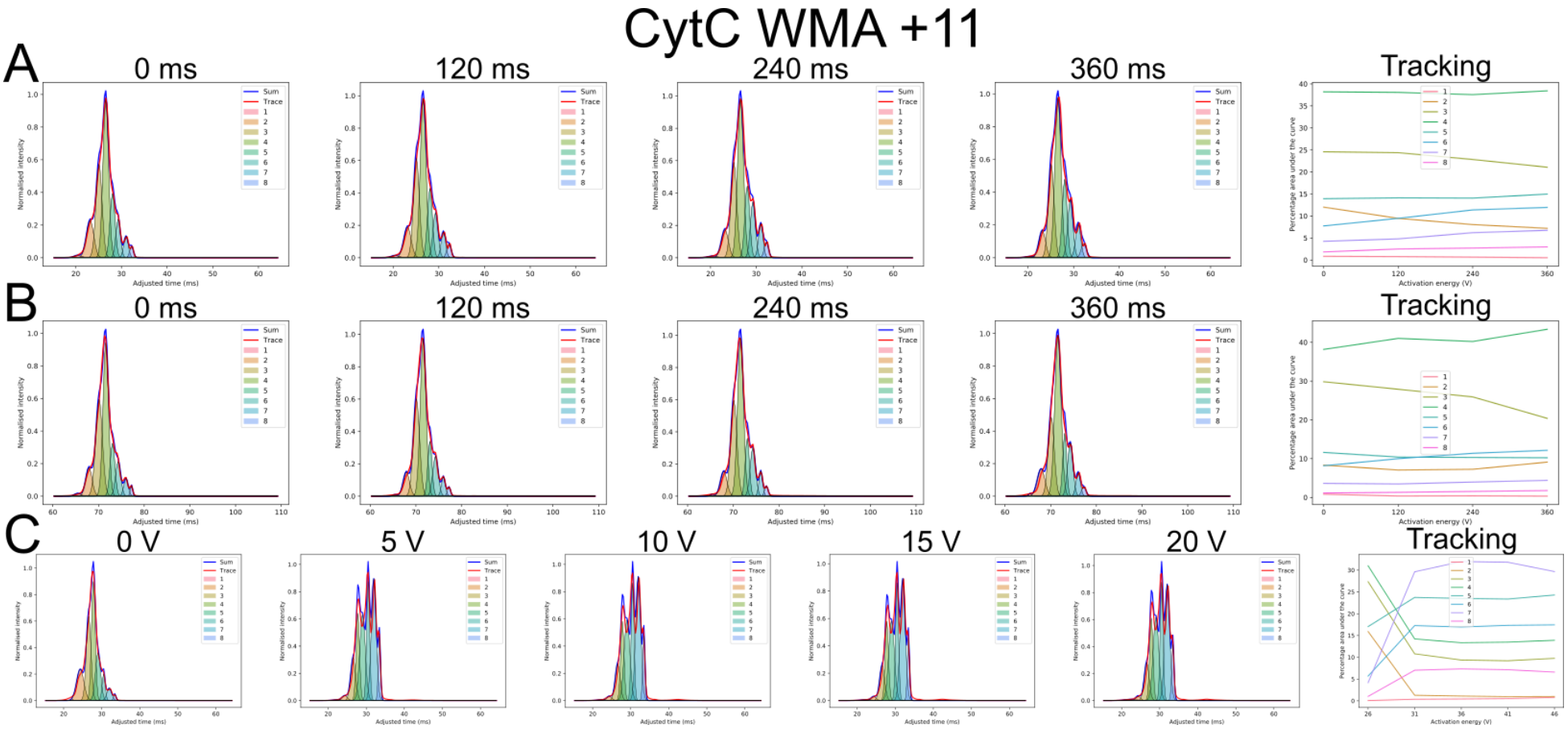

Figure S10 Population tracking for CytC WMA +11 experiments A) tracking B) spinning C) CIU

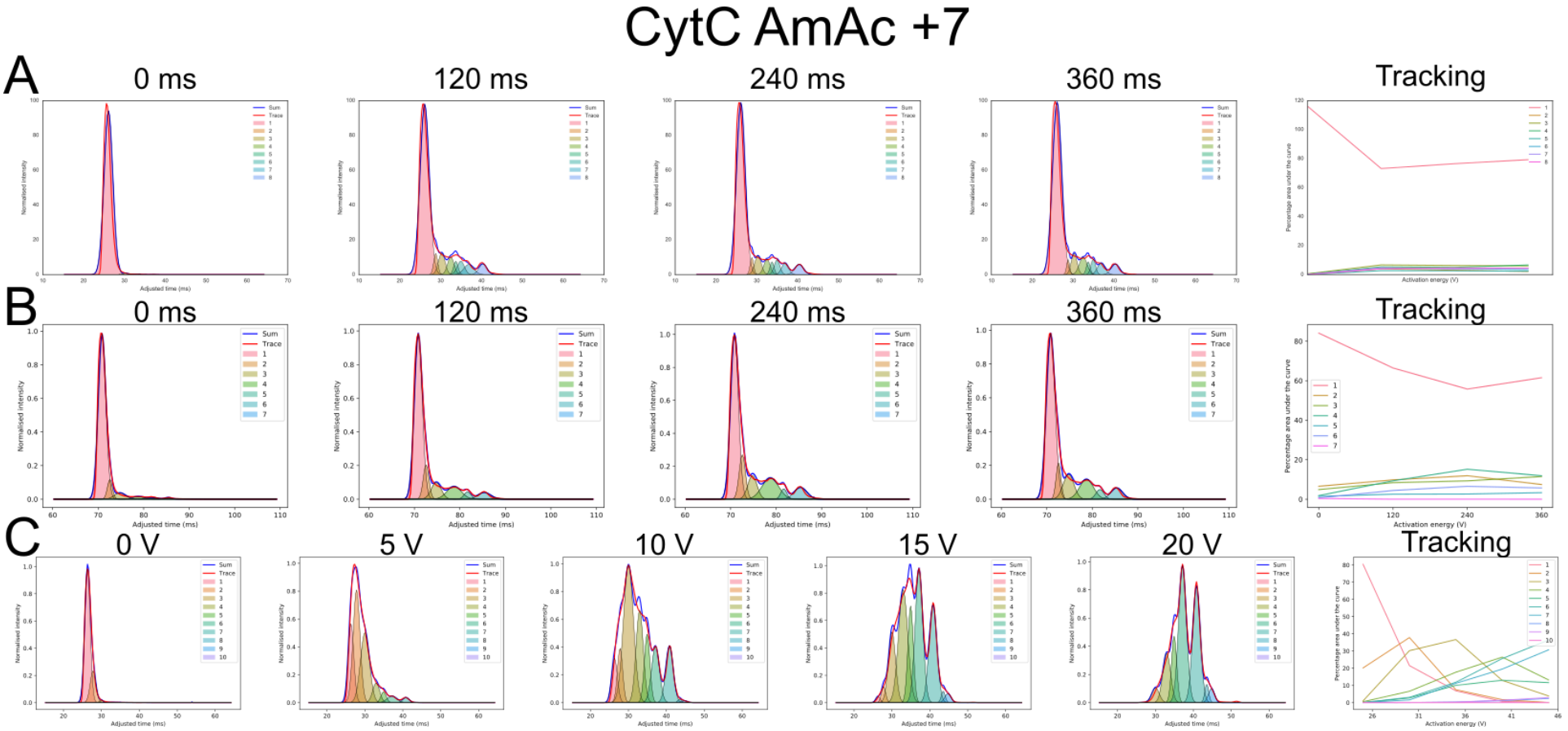

Figure S11 Population tracking for CytC WMA +11 experiments A) tracking B) spinning C) CIU

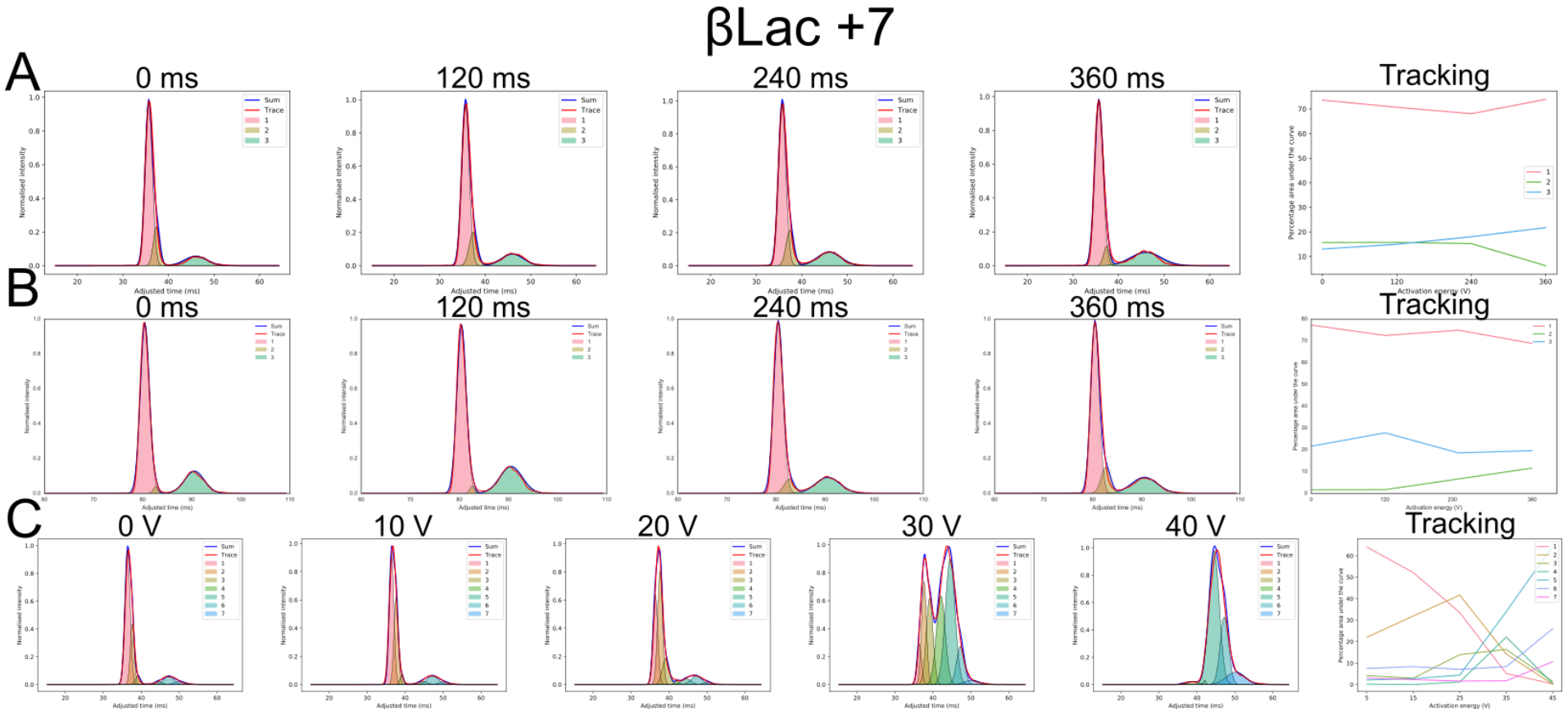

Figure S12 Population tracking for Blac +7 experiments A) tracking B) spinning C) CIU

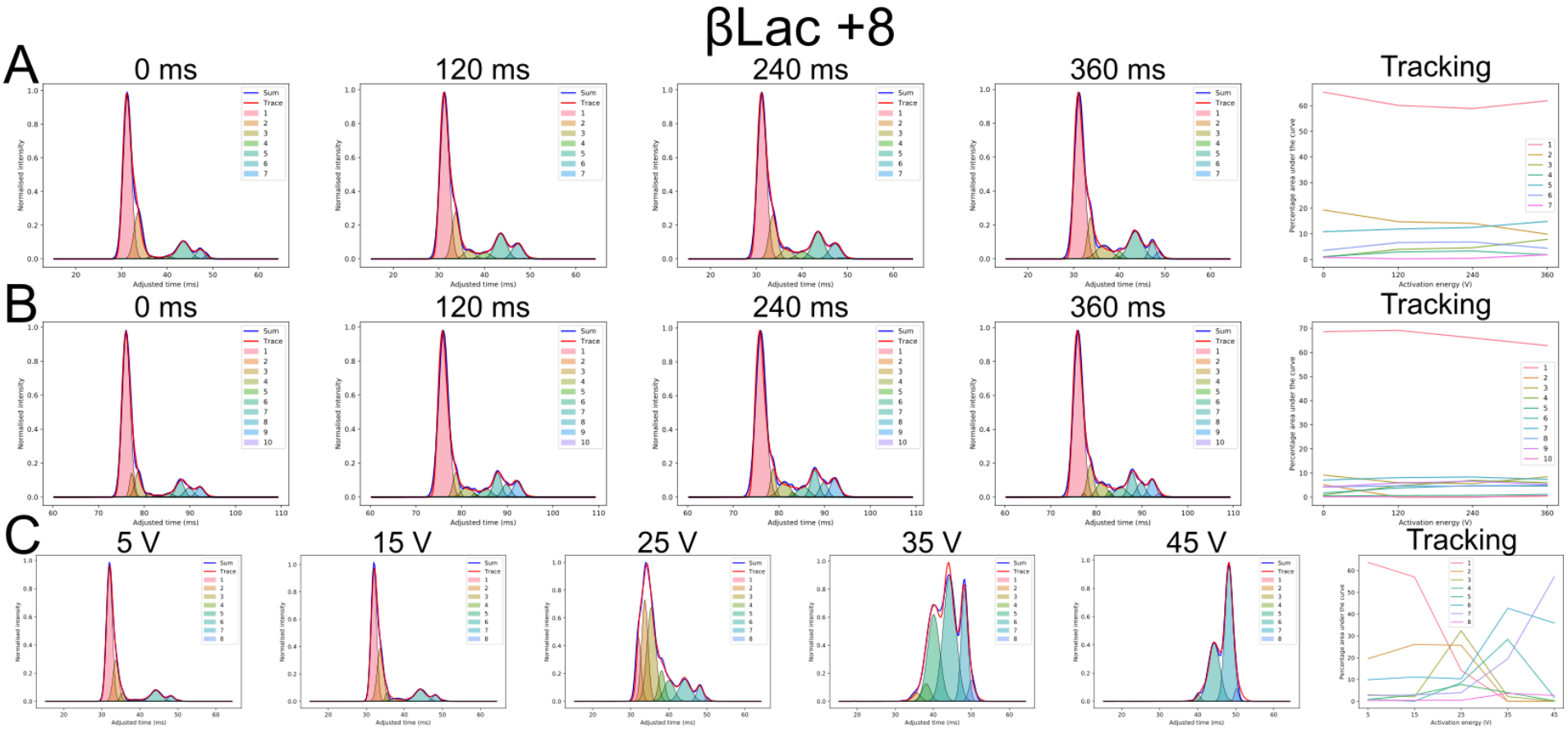

Figure S13 Population tracking for Blac +8 experiments A) tracking B) spinning C) CIU

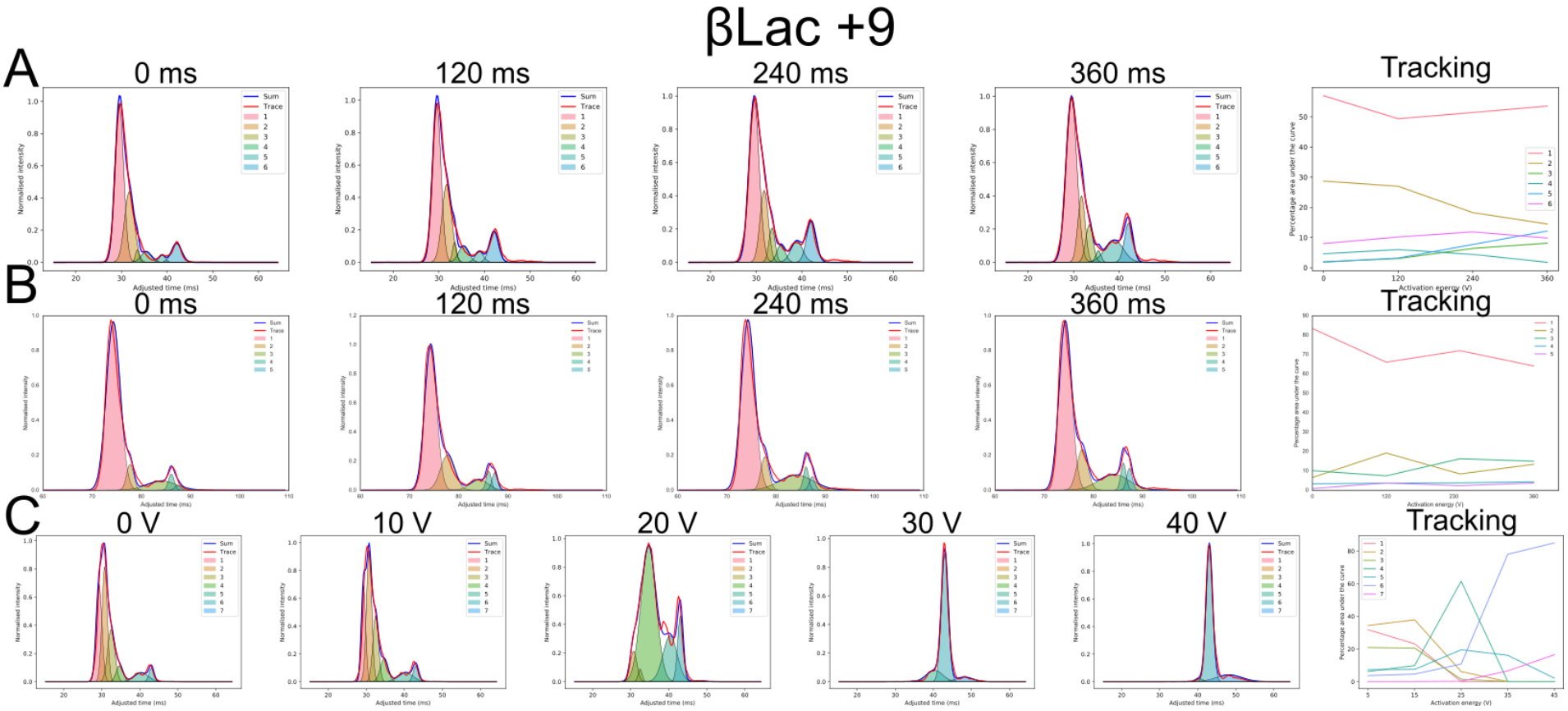

Figure S14 Population tracking for Blac +9 experiments A) tracking B) spinning C) CIU

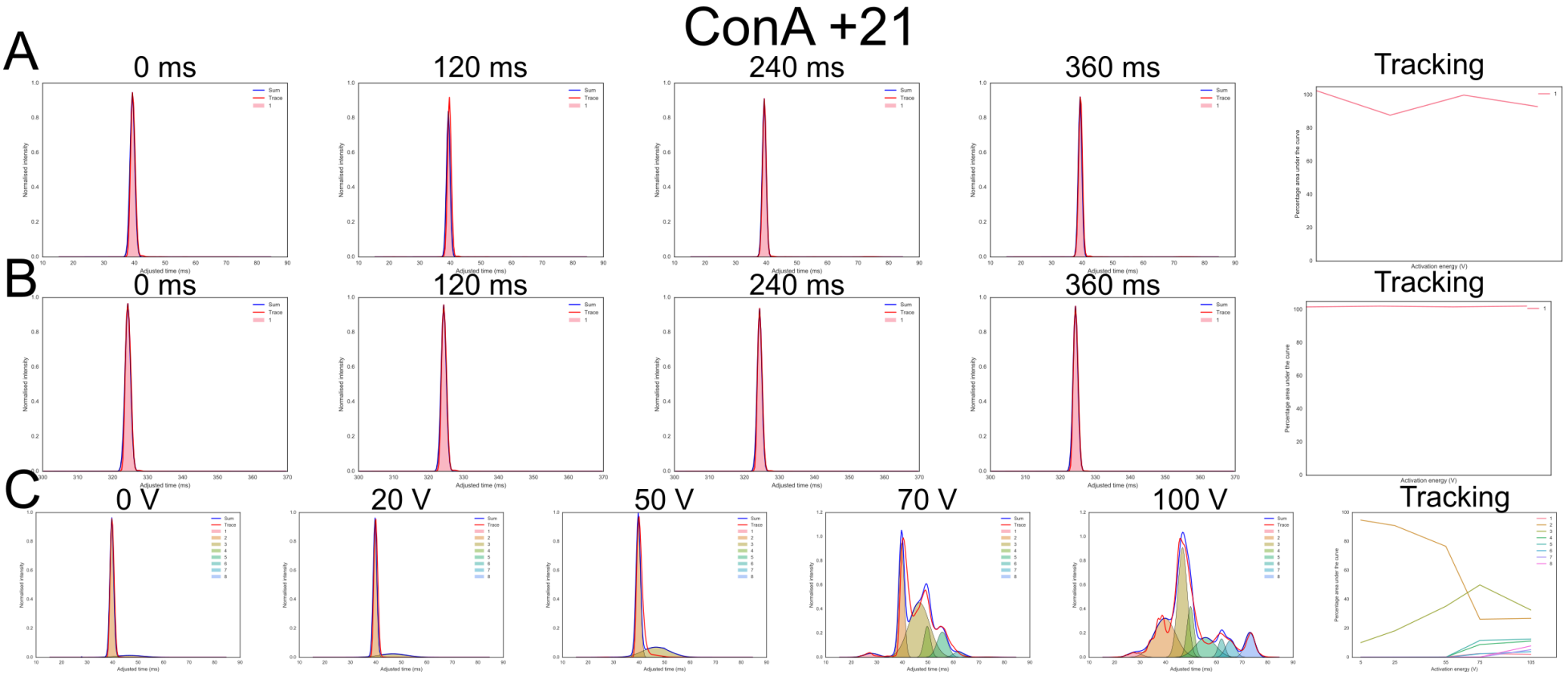

Figure S15 Population tracking for ConA+21 experiments A) tracking B) spinning C) CIU

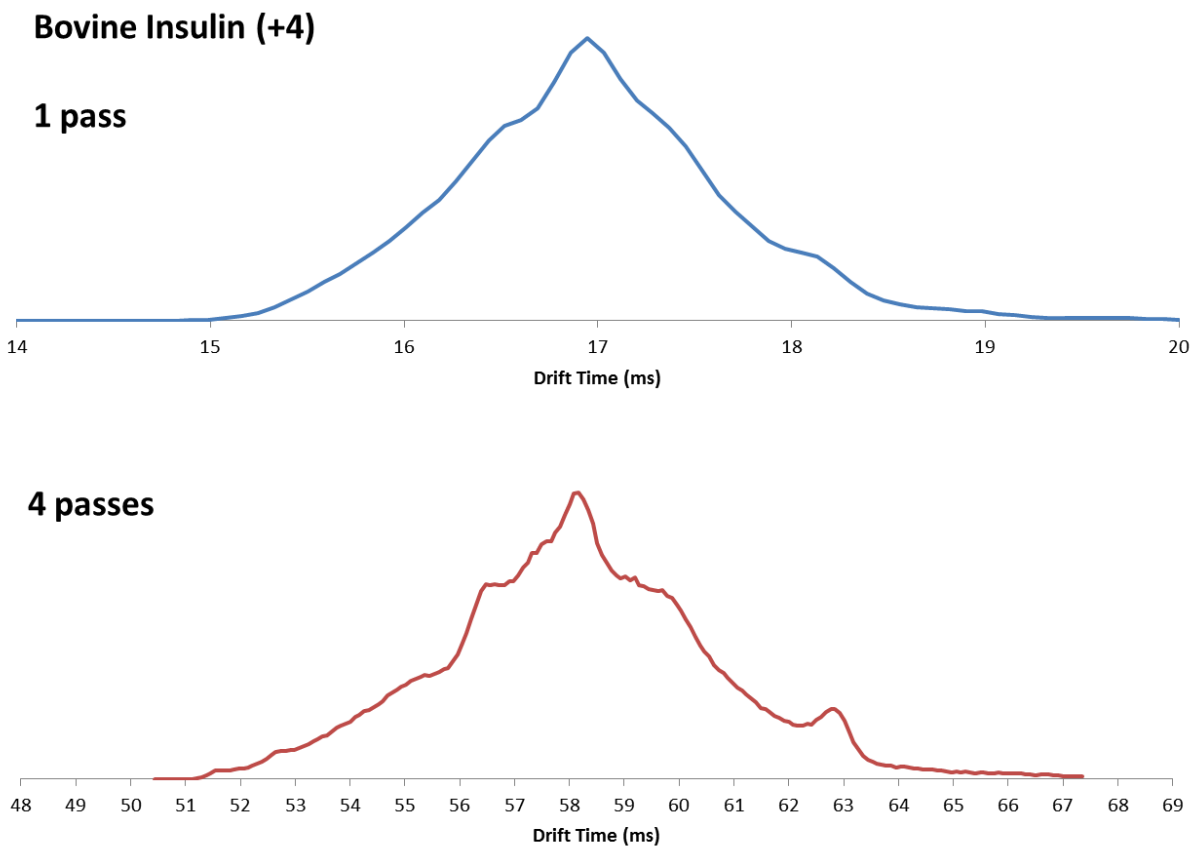

Figure S26 Bovine insluin after 1 pass and 4 passes (compressed) in the cIM. Conformations become more distinct after multiple passes.